



TTI1 promotes non-small-cell lung cancer progression by regulating the mTOR signaling pathway

Ling-Xian Zhang | Xin Yang | Zhi-Bo Wu | Zhong-Min Liao | Ding-Guo Wang | Shi-Wei Chen | Feng Lu | Yong-Bing Wu  | Shu-Qiang Zhu 

Department of Cardiothoracic Surgery,
The Second Affiliated Hospital of
Nanchang University, Nanchang, China

Correspondence

Shu-Qiang Zhu, Department of
Cardiothoracic Surgery, The Second
Affiliated Hospital of Nanchang
University, 1 Ming de Road, Nanchang,
Jiangxi, China.
Email: zsq276446377@163.com

Funding information

Jiangxi Provincial Department of Science
and Technology, Grant/Award Number:
20213BCJL22048; National Natural
Science Foundation of China, Grant/
Award Number: 81860520

Abstract

The role of TELO2-interacting protein 1 (TTI1) in the progression of several types of cancer has been reported recently. The aim of this study was to estimate the expression and potential value of TTI1 in non-small-cell lung cancer (NSCLC) patients. The expression of TTI1 and its prognostic value in NSCLC from The Cancer Genome Atlas (TCGA) database and Gene Expression Omnibus (GEO) database were analyzed. To verify the bioinformatics findings, a tissue microarray containing 160 NSCLC and paired peritumoral tissues from NSCLC patients was analyzed by immunohistochemistry for TTI1. Subsequently, the roles of TTI1 in NSCLC cells were investigated in vivo by establishing xenograft models in nude mice and in vitro by transwell, CCK-8, wound healing, and colony formation assays. In addition, quantitative real-time polymerase chain reaction and western blot were applied to explore the underlying mechanism by which TTI1 promotes tumor progression. Finally, the relationship between TTI1 and Ki67 expression level in NSCLC was probed, and Kaplan–Meier and Cox analyses were performed to assess the prognostic merit of TTI1 and Ki67 in NSCLC patients. We found that the expression of TTI1 was significantly upregulated in NSCLC tissues compared to paired peritumoral tissues, which coincides with the bioinformatics findings from the TCGA and GEO databases. TTI1 was highly expressed in NSCLC patients with large tumors, advanced tumor stage, and lymphatic metastasis. In addition, the prognostic analysis identified TTI1 as an independent indication for poor prognosis of NSCLC patients. In vitro, upregulation of TTI1 in NSCLC cells could facilitate cell invasion, metastasis, viability, and proliferation. Mechanistically, our study verified that TTI1 could regulate mTOR activity, which has a pivotal role in human cancer. Consistently, the expressions of TTI1 and Ki67 had a positive relationship in NSCLC cells and tissues. Notably, patients with overexpression of TTI1 or Ki67 had a shorter overall survival rate and a higher disease-free survival rate compared to patients with low expression of TTI1 or Ki67, and the combination of TTI1 and Ki67 was an independent parameter predicting the prognosis and recurrence of NSCLC patients. We conclude that TTI1 promotes NSCLC cell proliferation, metastasis, and

Ling-Xian Zhang, Xin Yang, and Zhi-Bo Wu contributed equally to this work.

This is an open access article under the terms of the [Creative Commons Attribution-NonCommercial-NoDerivs](https://creativecommons.org/licenses/by-nc-nd/4.0/) License, which permits use and distribution in any medium, provided the original work is properly cited, the use is non-commercial and no modifications or adaptations are made.

© 2022 The Authors. *Cancer Science* published by John Wiley & Sons Australia, Ltd on behalf of Japanese Cancer Association.

invasion by regulating mTOR activity, and the combination of TTI1 and Ki67 is a valuable molecular biomarker for the survival and recurrence of NSCLC patients.

KEYWORDS

biomarker, Ki67, mTOR, NSCLC, TELO2-interacting protein 1 (TTI1)

1 | INTRODUCTION

Lung cancer remains one of the most frequent malignancies and is the leading cause of cancer-related deaths worldwide.¹ Non-small-cell lung cancer (NSCLC) is the major pathological type of lung cancer, accounting for about >80% of the whole cohort.² Despite much progress having been made recently for NSCLC, such as minimally invasive techniques for diagnosis and treatment, targeted therapies, and immunotherapies, the overall 5-year survival rate of all NSCLC patients is only approximately 15%, and most postoperative patients may have early tumor recurrence.³ Thus, further investigation into the mechanism associated with cancer progression and recurrence is extremely urgent.

TELO2-interacting protein 1 (TTI1), also known as KIAA0406 or SMG10, is a member of the Triple T complex (TTT) that is composed of TELO2, TTI1, and TTI2.⁴ TTI1 is highly conserved throughout evolution and has homology in mice, chickens, flies, frogs, fish, plants, and yeast. The TTT complex works synergistically with heat shock protein 90 to maintain the function of the phosphatidylinositol 3-kinase-related protein kinase (PIKK) family of proteins.⁵ mTOR, a serine/threonine kinase and member of the PIKK family, regulates translation, cell growth, autophagy, and other processes, and plays an important role in human cancer.⁶ TTI1 is an mTOR-interacting protein that interacts with and stabilizes all six members of the PIKK family of proteins (mTOR, ataxia telangiectasia-mutated [ATM], ATM- and Rad3-related [ATR], DNA-dependent protein kinase catalytic subunit [DNA-PKcs], suppressor with morphological effect on genitalia 1 [SMG-1], and transformation/transcription domain-associated protein [TRRAP]).⁷ TTI1 participates in important biological functions. TTI1 and its binding partner Tel2 positively regulate mTOR activation and are involved in cell growth and metabolism.⁷ TTI1 via its C-terminus binds with IP6K2 and participates in the signaling pathway of p53-associated cell death mediated by IP6K2.⁸ In multiple myeloma, SCFFbxo9 targets Tel2 and Tti1 for degradation within mTORC1, and mTORC1 is inactivated to restrain cell growth and protein translation.⁹ As mentioned above, TTI1 may be involved in oncogenesis and progression of NSCLC, and further study is necessary.

In this study, we analyzed TTI1 expression and its prognostic value within NSCLC patients using a bioinformatics method. A tissue microarray (TMA) was analyzed to verify the bioinformatics findings that TTI1 was significantly upregulated in NSCLC tissues and is closely associated with the poor prognosis of NSCLC patients. Additionally, we identified that TTI1 could promote the progression of NSCLC. Mechanistically, our study verified the regulation of the

mTOR signaling pathway by TTI1. Subsequently, the relationship between the expression of TTI1 and/or Ki67 and the clinicopathological characteristics of NSCLC patients were further studied. Finally, we analyzed the relationship between the expression of TTI1 and Ki67, and the prognosis and recurrence of NSCLC patients.

2 | METHODS

2.1 | Expression data sets

Seven human lung cancer cohorts and corresponding clinical information were extracted from the Gene Expression Omnibus (GEO; GSE19188, GSE40791, GSE75037, GSE41271, GSE50081, and GSE31210) and The Cancer Genome Atlas (TCGA) database to analyze the expression of TTI1.

2.2 | Patients and follow-up

A total of 160 NSCLC tissues and matched nontumor tissues were gathered from patients who underwent surgery at The Second Affiliated Hospital of Nanchang University. The pathological diagnosis was carried out by two pathologists, independently, in accordance with the standards of the World Health Organization. The tissues were constructed into a TMA that was used to perform immunohistochemistry (IHC) staining. Clinicopathological information was collected from March 12, 2009 to February 28, 2011. The last follow-up was in December 2019. All patients had written informed consent regarding the collection and use of their tissue samples. The ethical approval was authorized by The Second Affiliated Hospital of Nanchang University. Disease-free survival (DFS) was defined as the time from tumor resection to disease recurrence or death due to disease progression. Overall survival (OS) was defined as the time from tumor resection to death from any cause. First progression (FP) was defined as the time from tumor resection to the first occurrence of disease progression or death from any cause. Postprogression survival (PPS) was defined as the time from progression to death after tumor resection. The definition of NSCLC differentiation is as follows.

Lung squamous cell carcinoma (LUSC). Well: Cancer cells are arranged in layers, with obvious keratin pearls, intracellular keratinization, and well-developed intercellular bridges in cancer nests. Moderate: The demarcation of the cancer cells is still clear, the nuclei around the cancer nest are arranged in a grid, and there are

intracellular keratinization and individual keratinized beads. Poor: The size of cancer cells varies, the intercellular bridge is not obvious, the nuclear atypia is obvious, and the mitoses are often accompanied by necrosis.

Lung adenocarcinoma (LUAD). Well: The glandular epithelium is arranged in tubular, papillary, and alveolar shapes, with no obvious cell atypia and rare mitoses. Poor: The tumor cells are in sheets and parenchyma, and there are only a few adenoid structures or mucus secretions. Moderate: This is in between well and poor.

2.3 | TMA establishment and IHC

TMA of 160 pairs of NSCLC tissues and matched nontumor tissues were built by Shanghai Biochip Co., Ltd. Rabbit polyclonal to human TTI1 antibody (1:200, ab234871; Abcam) and Rabbit polyclonal to human Ki67 antibody (1:200, ab16667; Abcam) were used to detect the expression of TTI1 and Ki67. The IHC assay was performed according to a standard protocol. In brief, after baking at 37 °C for 30 min, all paraffin sections of the human lung cancer tissues were first dewaxed and then rehydrated. Next, 5% BSA (YESEN) was incubated for 1 h at room temperature to block nonspecific binding sites. Then, the sections were incubated with primary antibodies overnight at 4 °C. Subsequently, endogenous peroxidase activity was blocked with incubation of the slides in 0.3% H₂O₂ at room temperature for 30 min, followed by incubation with secondary antibody for 1 h at room temperature. Next, the sections were stained with diaminobenzidine-H₂O₂ (Gene Tech) under a microscope and counterstained with hematoxylin. Finally, neutral balsam (Yeasen) was used to seal the slides with a cover slip. All assays included negative control slides without the primary antibodies. TTI1 staining was seen mainly in the cytoplasm of NSCLC and Ki67 was usually seen in the nucleus. The histochemistry score (H-score) was defined as the score for staining intensity multiplied by the score for staining percentage. According to the average intensity, the intensity was scored as follows: score 0 represents negative (0%–25%) intensity, score 1 represents weak (25%–50%) intensity, score 2 represents moderate (50%–75%) intensity, and score 3 represents strong (75%–100%) intensity. Based on the percentage of positive tumor cells, the percentage was scored as follows: score 1 indicates a negative (0%–25%) percentage, score 2 indicates a low (25%–50%) percentage, score 3 indicates a moderate (50%–75%) percentage, and score 4 indicates a high (75%–100%) percentage.

2.4 | Cell culture

The cell lines involved in this study included the human NSCLC cell lines A549, PC-9, NCI-H460, NCI-H1299, and the human bronchial epithelioid (HBE) cell, which were obtained from the Cell Bank of the Chinese Academy of Sciences. The cells were cultivated in DMEM or RPMI-1640 (Gibco) supplemented with 10% FBS (Gibco) and 1%

penicillin–streptomycin (Yeasen). The environmental conditions were 37 °C and 5% CO₂ in a humidified incubator.

2.5 | Total RNA extraction and qRT-PCR detection

Total RNA from cultured cells was extracted using the Trelief™ RNAprep FastPure Tissue & Cell Kit (Tsingke) and reverse transcribed into cDNA using a Hifair® III 1st Strand cDNA Synthesis Kit (gDNA digester plus) (Yeasen) according to the manufacturer's instructions. Subsequently, according to the manufacturer's protocol, quantitative real-time polymerase chain reaction (qRT-PCR) was performed with Hieff® qPCR SYBR Green Master Mix (High Rox Plus) (Yeasen). GAPDH was used as an internal reference gene for quantification of mRNA. The relative RNA level was calculated by using the 2^{-ΔΔCt} method. The RT-qPCR primers used in this study are as follows: TTI1, forward primer: AAGTCATGCTGCGGAAGTCA, reverse primer: TGGGAACCACTGGGCTAATG; mTOR, forward primer: CCAGGCCGCATTGTCTCTAT, reverse primer: AGTC TCTAGCGTGCCCTTTC; ribosomal protein S6 kinase beta-1 (S6K1), forward primer: CTGAGGACATGGCAGGAGTG, reverse primer: ACAATGTTCCATGCCAAGTTCA. EIF4EBP1, forward primer: CAAGG GATCTGCCACCATT, reverse primer: AACTGTGACTCTTCCCGCC. All experiments were done three times.

2.6 | Transfection experiment

The lentiviral vectors of TTI1 and shTTI1 were obtained from Genomeditech to construct stably transfected cell lines. The five shRNA target sequences are 5'-GCAGAACAGGAGAAATCAAAG-3', 5'-GGTCACAGCATTGTCGTATCT-3', 5'-GCAAG CTGCCATGATCC TTAA-3', 5'-CATTGTGCTATCTTCCCTAAA-3', and 5'-GCAGTCA ATCATTGGTGAAT-3'. The transfection efficiency was examined by western blotting and qRT-PCR.

2.7 | Colony formation and CCK-8 assay

The colony formation and the CCK-8 assay were employed to determine the cellular proliferation. For the colony formation assay, 1000 cells per well were cultured in a six-well plate (Corning) for 10 days. Then, all wells were rinsed with phosphate-buffered saline three times, fixed with 4% paraformaldehyde for 10 min, and stained with 0.4% crystal violet for 15 min. After rinsing with water and drying, all wells were photographed, and the total number of colonies was observed and counted. The results of three independent experiments were shown as mean ± standard deviation. For the CCK-8 assay, the Cell Counting Kit-8 (Yeasen) was purchased and used according to the manufacturer's protocol. First, we seeded cells in a 96-well plate (Corning) at approximately 1000 cells/well. Then, 10 μl of CCK-8 reagent was added to each well after 24, 48, and 72 h, the plates were incubated for 2 h, and the absorbance of all plates was measured at 450 nm.

2.8 | Wound healing, migration and transwell invasion assays

The wound healing assay and transwell assay (with Matrigel coating) were performed to detect cell invasion. For the wound healing assay, cells were seeded in a six-well plate (Corning) and cultured until confluent. Then, a (yellow) pipette tip was used to make a straight scratch, simulating a wound. Subsequently, the cells were photographed at 0, 24, and 48 h. For the transwell assay (with Matrigel coating) (BD Biosciences), the upper chamber was first coated with Matrigel and then 1×10^6 cells in serum-free medium were seeded into it before 500 μ l of culture medium containing 10% fetal bovine serum was added into the under chamber. After incubation for 36 h at 37 °C in a humidified atmosphere of 5% CO₂, the transwell chambers were fixed with 4% paraformaldehyde for 10 min and stained with 0.4% crystal violet for 15 min. Finally, the transwell chambers were rinsed, the upper cell layer from the filter was wiped with a cotton swab, and the cells were photographed under a microscope and counted.

2.9 | Western blot analysis

The procedures of the experiments were performed according to previous studies.^{10,11} In brief, cells were lysed with RIPA buffer (Beyotime) containing PMSF (Beyotime). The cell lysates were collected and centrifuged for 15 min at 12,000 \times g (4 °C). The supernatants were transferred to clean tubes, and SDS-PAGE sample loading buffer (Beyotime) was added. Then, they were boiled for 10 min and cooled down to room temperature. Proteins were subsequently separated on SDS-PAGE electrophoresis and then transferred onto PVDF membranes (Millipore). The membranes were blocked with protein-free rapid blocking buffer (Epizyme) and incubated overnight at 4 °C with primary antibodies. On the following day, the membranes were incubated with an HRP-conjugated secondary antibody for 1 h at room temperature and visualized with super ECL detection reagent (Yeasten) according to the manufacturer's instructions. The TTI1 (1:5000, ab176696; Abcam), p-mTOR(1:1000, ab109268; Abcam), mTOR(1:5000, ab134903; Abcam), p-S6K1 (1:1000, ab228513; Abcam), S6K1(1:1000; ab32359; Abcam), p-4EBP1 (1:1000, ab27792; Abcam), 4EBP1(1:2000; ab32024; Abcam), Tublin (1:1000, AF0001; Beyotime), and GAPDH (1:1000, AF0006; Beyotime) were used as primary antibodies.

2.10 | In vivo tumor growth

Immunodeficient nude mice (4–6 weeks of age) were purchased from Jiesijie and fed in a pathogen-free environment. The experiment was approved by the Animal Experimentation Ethics Committee of The Second Affiliated Hospital of Nanchang University. About 5×10^6 cells were resuspended in 150 μ l of DMEM and injected subcutaneously into the right side of the flank area of nude mice. Tumor volumes were calculated as $(\text{length} \times \text{width}^2)/2$ every 4 days.

2.11 | Statistical analysis

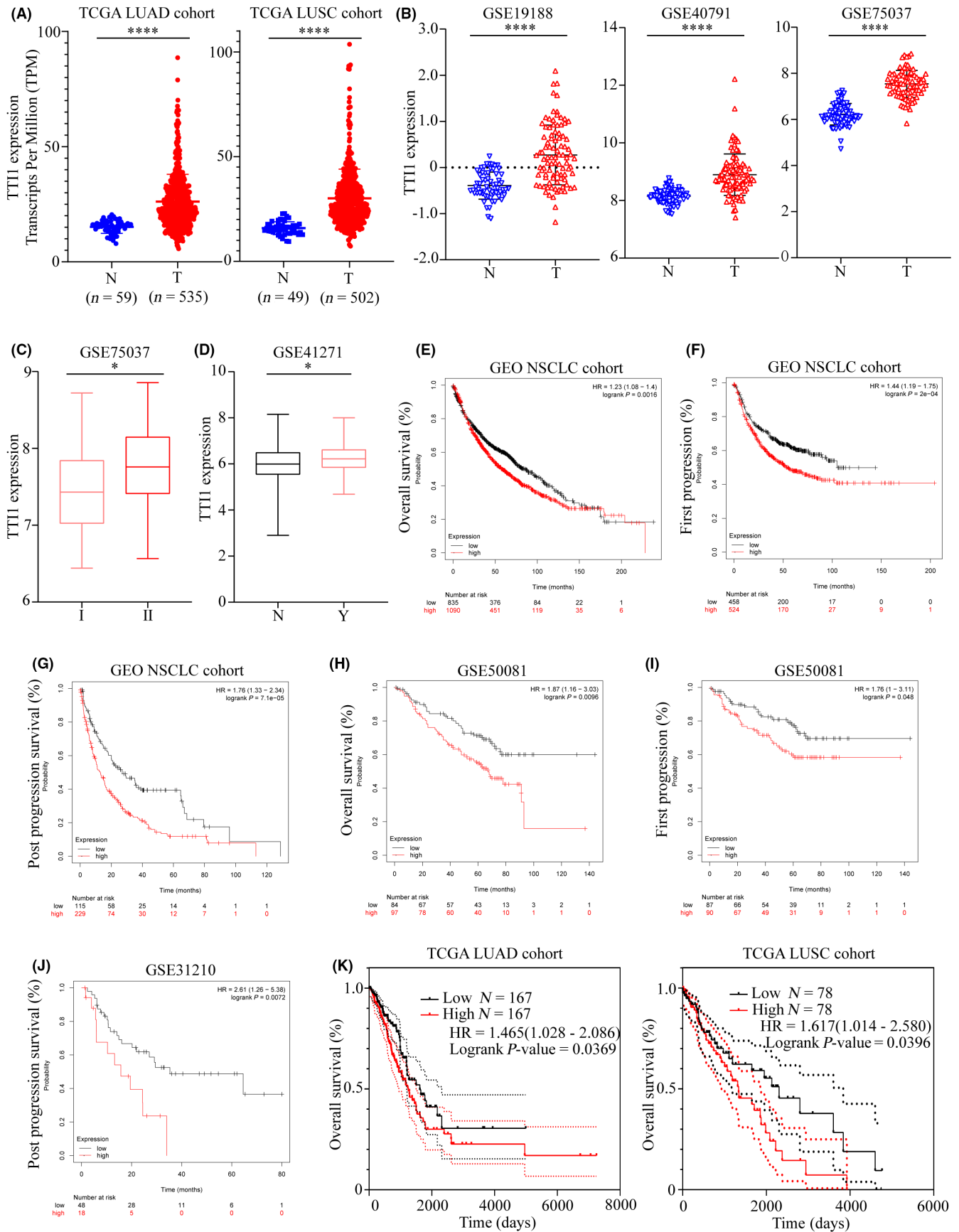
The SPSS 23.0 software program (IBM SPSS) was used for statistical calculations. The values are shown as the mean \pm standard deviation. Chi-squared or Fisher's exact tests were used to compare the categorical variables, and Student's *t* test was chosen to compare the difference in measurement data between two groups. A Spearman correlation analysis was used to detect the correlation between the expression of TTI1 and Ki67. The best cut-off value of TTI1 and Ki67 expressions was divided by X-tile software.¹² The OS and DFS analyses were estimated by the Kaplan–Meier method, and the comparison was evaluated by the log-rank test. The univariate and multivariate analyses were conducted using a model of Cox's proportional hazards regression. $P < 0.05$ was regarded as statistically significant.

3 | RESULTS

3.1 | Expression of TTI1 mRNA was significantly upregulated and a high level of TTI1 mRNA predicts unfavorable prognosis in NSCLC

Based on TCGA analysis, TTI1 mRNA expression was significantly upregulated in LUAD and LUSC compared to normal lung tissues (Figure 1A), and a similar result was discovered in three independent GEO NSCLC cohorts (Figure 1B). Furthermore, we found that there was a significant positive correlation between the TTI1 mRNA and the advanced TNM stage (Figure 1C). The expression of TTI1 mRNA in patients with recurrence was significantly higher than in those without (Figure 1D). To investigate the prognostic value of TTI1 mRNA, we analyzed the OS, FP, and PPS rates in the GEO NSCLC cohort and two additional independent GEO cohorts (GSE50081 and GSE31210). Kaplan–Meier analysis showed that the OS, FP, and

FIGURE 1 Expression of TELO2-interacting protein 1 (TTI1) mRNA in non-small-cell lung cancer (NSCLC) and its prognostic significance based on bioinformatic analysis. (A) The expression levels of TTI1 were analyzed in lung adenocarcinoma (LUAD) and lung squamous cell carcinoma (LUSC) tissues from The Cancer Genome Atlas (TCGA) databases. (B) Expression of TTI1 in three independent Gene Expression Omnibus (GEO) datasets. (C) TTI1 expression in clinical TNM stages I and II, respectively. (D) TTI1 expression in no or yes recurrence. (E) Overall survival (OS), (F) first progression (FP), and (G) postprogression survival (PPS) rate analysis of the NSCLC patients based on GEO databases. (H) OS, (I) FP, and (J) PPS rate analysis of the NSCLC patients in GSE50081 and GSE31210. (K) OS rate analysis of LUAD and LUSC patients based on TCGA databases. The data are presented as mean \pm SD. * $P < 0.05$, **** $P < 0.0001$



PPS times of patients with high expression of TTI1 mRNA were significantly shorter than those of patients with low expression of TTI1 mRNA in almost all NSCLC cohorts (Figure 1E-J). The same result (OS)

was verified in TCGA LUAD and LUSC cohorts (Figure 1K). Overall, these results indicate that TTI1 mRNA is significantly upregulated and may represent a new prognostic biomarker for NSCLC patients.

3.2 | TTI1 protein levels were also upregulated and positively associated with tumorigenic phenotypes of NSCLC patients

Furthermore, TMAs of 160 pairs of NSCLC tissues and matched nontumor tissues were used to validate the dysregulated TTI1 expression in NSCLC at the protein level. The results showed that the expression of TTI1 in NSCLC tissues was significantly higher than that in noncancerous tissues (Figure 2A). Moreover, we found that high TTI1 expression was significantly correlated with larger tumor size, advanced TNM stage, and lymph node metastasis (Figure 2B–D). Patients with advanced TNM stage had poor OS and DFS (Figure S1A,B). The TTI1 protein was mostly located in the cytoplasm (Figure 2E). The X-tile software was used to divide the best cutoff value to distinguish TTI1^{high} and TTI1^{low} groups of 160 NSCLC specimens. As shown in Table 1, TTI1^{high} was significantly correlated with larger tumor size ($P = 0.003$), advanced TNM stage ($P = 0.008$), and lymph node metastasis ($P = 0.043$), while the other clinical characteristics, including age, gender, smoking history, histological type, and differentiation, were not significantly related to TTI1 expression. Furthermore, univariate and multivariate analysis validated that TTI1 expression, TNM stage, and lymph node metastasis were independent predictors of OS (Table 2), and TTI1 expression, TNM stage, and differentiation were independent predictors of DFS (Table 3) in patients with NSCLC. In summary, these findings strongly indicate that the high expression of TTI1 was positively correlated with poor prognosis and might serve as a prognostic biomarker for patients with NSCLC.

3.3 | TTI1 promotes NSCLC cell metastasis, invasion, and proliferation in vitro

Considering the above findings, the impact of TTI1 on the biological function of NSCLC was further investigated. The mRNA and protein expression of TTI1 in HBE cells and three NSCLC cell lines were detected by qRT-PCR and western blot, respectively, and the results showed that TTI1 was highly expressed in NSCLC cell lines compared with normal lung cells at both the mRNA and protein levels, and was expressed at the highest level in A549 cells and at the lowest level in H460 cells in the three NSCLC cell lines (Figure 3A,B). Five short hairpin RNAs and two overexpression plasmids were investigated, and those showing the strongest knockdown effects (shRNA1 and shRNA5) or overexpression effects (TTI1-1 and TTI1-2) were chosen for subsequent experiments. Thus, TTI1 was knocked down in A549 cells (A549-shTTI1-1, A549-shTTI1-5) and overexpressed in H460 cells (H460-TTI1-1, H460-TTI1-2) by the lentivirus transduction method, generating four stable cell lines (Figure 3C,D). The CCK-8 and colony formation assays showed that the proliferation ability was decreased after the knockdown of TTI1 and increased on the up-regulation of TTI1 in NSCLC cells (Figure 3E,F). The wound healing

assay indicated that the migration capacity of A549-shTTI1-1 and A549-shTTI1-5 cells was impaired and that of H460-TTI1-1 and H460-TTI1-2 cells was enhanced (Figure 3G). Consistently, the Matrigel transwell assay revealed that the invasion capacity of NSCLC cells in TTI1 knocked down groups was significantly reduced compared with the control group and, on the contrary, the invasion capacity was markedly improved in the TTI1 upregulated groups compared with the control group (Figure 3H). Collectively, these results indicate the crucial role of TTI1 in regulating NSCLC cell growth and metastasis.

3.4 | TTI1 regulates the mTOR signaling pathway and promotes NSCLC progression in vivo

We further revealed the underlying mechanism by which TTI1 promotes the progression of NSCLC. Initially, we used publicly available data (STRING, <https://cn.string-db.org/>) to find the protein–protein interaction networks of TTI1 and found that a total of 20 proteins have close interactions with TTI1 (Figure 4A). The database had performed Kyoto Encyclopedia of Genes and Genomes (KEGG) analysis to explore TTI1-related downstream pathways and we made a bubble chart (Figure 4B). From the KEGG analysis, we speculated that TTI1 regulates the mTOR signaling pathway in NSCLC. Hence, we detected mTOR and downstream signaling proteins, including S6K1 and 4EBP1, in NSCLC cell lines at mRNA and protein levels. We found that mTOR, S6K1, and 4EBP1 of both A549-shTTI1-1, A549-shTTI1-5 and H460-TTI1-1, H460-TTI1-2 showed no change at mRNA and protein levels. However, p-mTOR, p-S6K1, and p-4EBP1 of A549-shTTI1-1 and A549-shTTI1-5 were significantly reduced compared with the control group. Conversely, p-mTOR, p-S6K1, and p-4EBP1 of H460-TTI1-1 and H460-TTI1-2 were markedly improved compared with the control group (Figure 4C–E). Those findings demonstrate that TTI1 regulates the mTOR signaling pathways in NSCLC. Finally, the in vivo assay in nude mice subcutaneously implanted with A549-shTTI1-1, A549-shTTI1-5, H460-TTI1-1, H460-TTI1-2, and control cells further identified that the knockdown of TTI1 could impair the progression of NSCLC and the overexpression of TTI1 could accelerate the growth of NSCLC (Figures 4F–H and S2A–C).

3.5 | The TTI1 biological function of NSCLC cells could be reversed by the mTOR kinase inhibitor AZD5088

AZD5088, an ATP-competitive inhibitor of mTOR kinase activity with an IC₅₀ of 0.8 nmol/L, has been shown in vitro and in vivo to inhibit proliferation, migration, and invasion in numerous human tumor cells.^{13–15} Our study revealed that TTI1 could promote NSCLC progression by regulating the mTOR signaling pathway. To confirm the importance of the TTI1–mTOR axis, we examined the efficacy of mTOR inhibitor AZD5088 on cell growth and invasion

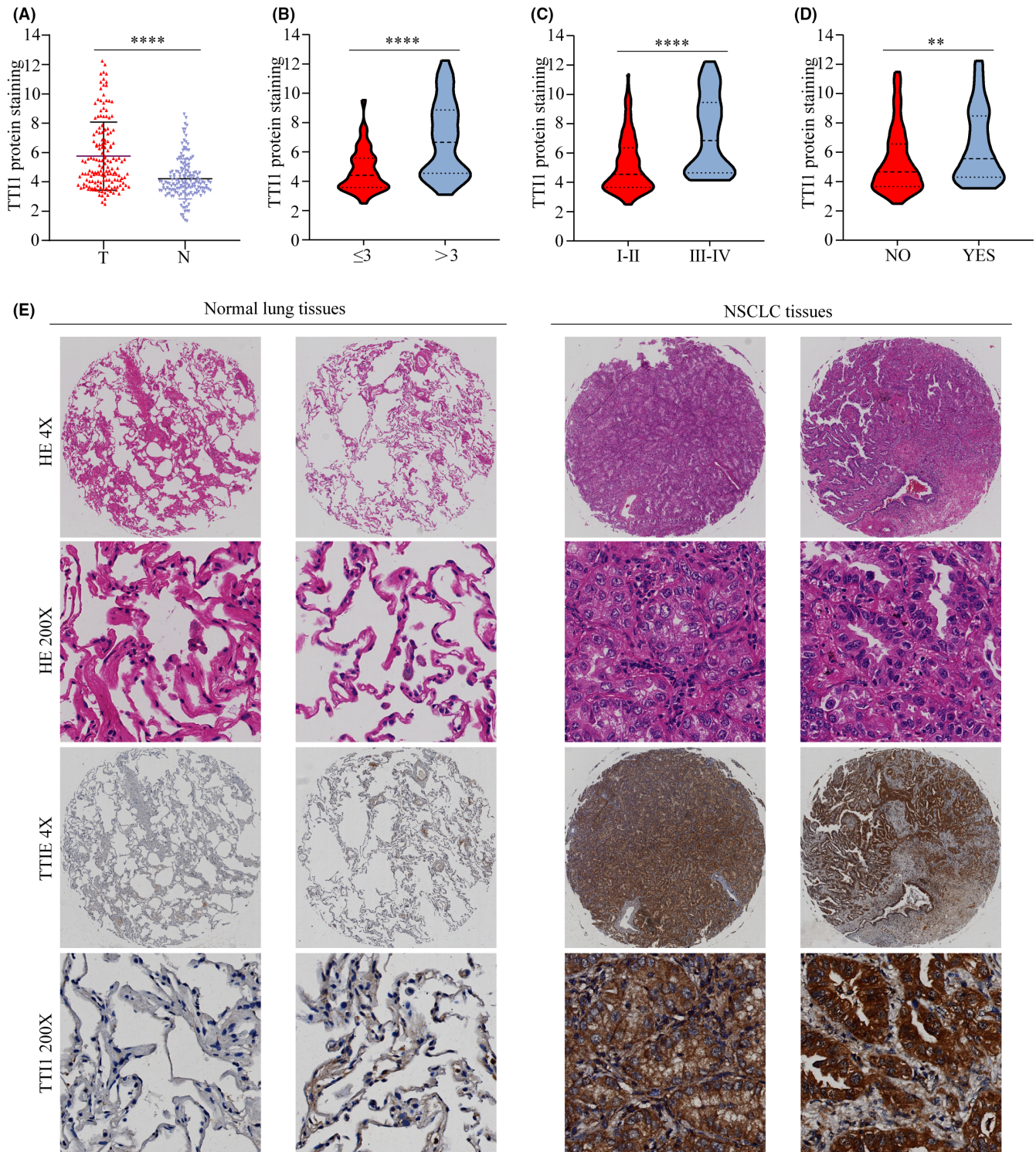


FIGURE 2 Expression of TELO2-interacting protein 1 (TTI1) protein level and its association with malignant phenotypes in non-small-cell lung cancer (NSCLC) patients. (A) TTI1 protein expression levels in NSCLC and noncancerous tissues. (B–D) The expression of TTI1 was analyzed according to the tumor diameter (≤ 3 cm vs. > 3 cm), TNM stage (I–II vs. III–IV) and lymph node metastasis status (yes vs. no). (E) Representative images of TTI1 expression in NSCLC tissues of serial sections stained with H&E and immunohistochemistry. The data are presented as mean \pm SD of three independent experiments. ** $P < 0.01$, **** $P < 0.0001$

of NSCLC cells with or without TTI1 expression. We found that the protein levels of mTOR, S6K1, and 4EBP1 in A549, A549-shTTI1-5, H460, and H460-TTI1-2 had no change after treatment with AZD5088 (20 ng/ml) for 24 h. However, the protein levels of

p-mTOR, p-S6K1, and p-4EBP1 in A549, A549-shTTI1-5, H460, and H460-TTI1-2 were all reduced compared with the DMSO treatment group (Figure S3A), which indicates that the high level of TTI1 did not influence the expression of mTOR, S6K1, and 4EBP1

Clinicopathological parameters	TTI1 ^{Low}	TTI1 ^{High}	P value	Ki67 ^{Low}	Ki67 ^{High}	P value
Age						
<60	48	45		51	42	
≥60	38	29	0.523	43	24	0.236
Gender						
Male	37	42		48	31	
Female	49	32	0.083	46	35	0.610
Smoking history						
Smokers	30	32		36	26	
Nonsmokers	56	42	0.279	58	40	0.889
Histological type						
Squamous	35	36		45	26	
Adenocarcinoma	51	38	0.313	49	40	0.288
Tumor stage						
I–II	69	46		77	38	
III–IV	17	28	0.011	17	28	0.001
Lymph node metastasis						
No	64	44		70	38	
Yes	22	30	0.044	24	28	0.025
Tumor size						
<3 cm	53	30		57	26	
≥3 cm	33	44	0.008	37	40	0.008
Differentiation						
Well and moderate	45	30		55	20	
Poor	41	44	0.136	39	46	0.0004

TABLE 1 Correlations between TELO2-interacting protein 1 (TTI1) or Ki67 and clinical characteristics in 160 non-small-cell lung cancer patients

TABLE 2 Univariate and multivariate analyses of factors associated with overall survival

Factors	OS			
	Univariate, P	HR	95% CI	P value
Age (<60 vs. ≥60)	0.481			NA
Gender (female vs. male)	0.29			NA
Smoking history (smokers vs. nonsmokers)	0.677			NA
Histological type (SCC vs. adenocarcinomas)	0.894			NA
Tumor stage (III–IV vs. I–II)	0.004	1.717	1.062–2.775	0.027
Lymph node metastasis (yes vs. no)	0.002	1.66	1.025–2.689	0.039
Tumor size (>3 cm vs. ≤3 cm)	0.012			NS
Differentiation (poor vs. well and moderate)	0.008			NS
TTI1 expression (high vs. low)	0.005	1.576	1.329–2.152	0.007
Ki67 expression (high vs. low)	<0.001	1.727	1.298–2.721	<0.001
TTI1 and Ki67 expression (TTI1 and Ki67 high vs. others*)	<0.001	1.921	1.196–3.086	<0.001

Note: Cox proportional hazards regression model; TTI1 and Ki67 high, TTI1^{high} and Ki67^{high}; others* (TTI1^{low} and Ki67^{low}, TTI1^{high} and Ki67^{low}, TTI1^{low} and Ki67^{high}).

Abbreviations: 95% CI, 95% confidence interval; HR, hazard ratio; NA, not adopted; NS, not significantly; OS, overall survival; SCC, squamous cell carcinoma; TTI1, TELO2-interacting protein 1.

TABLE 3 Univariate and multivariate analyses of factors associated with cumulative recurrence

Factors	Cumulative recurrence			
	Univariate, <i>P</i>	HR	95% CI	<i>P</i> value
Age (<60 vs. ≥60)	0.952			NA
Gender (female vs. male)	0.508			NA
Smoking history (smokers vs. nonsmokers)	0.431			NA
Histological type (SCC vs. adenocarcinomas)	0.416			NA
Tumor stage (III–IV vs. I–II)	≤0.001	1.719	1.122–2.636	0.013
Lymph node metastasis (yes vs. no)	0.048			NS
Tumor size (>3 cm vs. ≤3 cm)	0.045			NS
Differentiation (poor vs. well and moderate)	≤0.001	1.72	1.147–2.579	0.009
TTI1 expression (high vs. low)	0.002	1.395	1.054–2.081	0.042
Ki67 expression (high vs. low)	<0.001	1.484	1.067–2.137	0.009
TTI1 and Ki67 expression (TTI1 and Ki67 high vs. others*)	<0.001	1.675	1.310–2.450	<0.001

Note: Cox proportional hazards regression model; TTI1 and Ki67 high, TTI1^{high} and Ki67^{high}; others* (TTI1^{low} and Ki67^{low}, TTI1^{high} and Ki67^{low}, TTI1^{low} and Ki67^{high}). Abbreviations: 95% CI, 95% confidence interval; HR, hazard ratio; NA, not adopted; NS, not significantly; OS, overall survival; SCC, squamous cell carcinoma; TTI1, TELO2-interacting protein 1.

mRNA and protein levels, but only affected the phosphorylation of these molecules. The colony formation assay showed that viability of A549, A549-shTTI1-5, H460, and H460-TTI1-2 all decreased after AZD5088 treatment (Figure S3B). The CCK-8 assay revealed that following treatment with AZD5088, the proliferation of A549, A549-shTTI1-5, H460, and H460-TTI1-2 all reduced (Figure S3C). The Matrigel transwell assay and the wound healing assay indicated that, compared with the DMSO treatment group, the invasion and the migration capacity of A549, A549-shTTI1-5, H460, and H460-TTI1-2 were dramatically reduced (Figure S3D,E). Consequently, our findings demonstrated that AZD5088 inhibited the TTI1-mTOR axis signaling pathway.

3.6 | The level of TTI1 had a positive correlation with the level of Ki67 in NSCLC patients

We used another publicly available dataset (GEPID 2 [cancer-pku.cn]) to conduct Pearson analysis of the correlation between TTI1 and Ki67 transcriptional expression, and found that TTI1 and Ki67 had a moderate correlation in LUAD ($R = 0.49$, $P = 0$) and in LUSC ($R = 0.34$, $P = 1.6 \times 10^{-14}$) (Figure 5A). Then, TMAs of 160 NSCLC tissues were used to analyze the expression of TTI1 and Ki67. According to the staining intensity of each specimen, TTI1 and Ki67 expressions were classified into four grades: negative, low, moderate, and strong (Figure 5B). Finally, Pearson analysis was conducted, and in accordance with the before bioinformatics analysis, it had a moderate correlation ($R = 0.5682$, $P < 0.0001$) between TTI1 and Ki67 protein expression (Figure 5C). These findings validated that TTI1 and Ki67 expression had a moderate correlation in NSCLC both at mRNA and protein levels.

3.7 | TTI1 combined with Ki67 was an independent parameter predicting the prognosis and recurrence of NSCLC patients

We showed that a high level of TTI1 promotes the progression of NSCLC mainly by inducing NSCLC cell proliferation. Moreover, a moderate correlation between TTI1 and Ki67 expression was found in NSCLC tissues. Thus, we speculated that TTI1 and Ki67 together might be more sensitive in predicting the prognosis and the relapse of NSCLC patients than Ki67 alone. Thus, we tried to analyze the clinical significance of TTI1, Ki67, and the combination of TTI1 and Ki67 on the prognosis and recurrence of NSCLC patients. The univariate and multivariate analyses validated the expression of TTI1, the expression of Ki67, and the expression of both TTI1 and Ki67 as independent predictors of OS and DFS in patients with NSCLC (Tables 2 and 3). At the last follow-up, the 2-year OS rates of the entire population was 86%, 5-year OS rates was 48.2%, 2-year DFS rates was 74.3%, and 5-year DFS rates was 35.3%. The TTI1 low group had significantly higher 2- and 5-year OS and DFS rates than the TTI1 high group ([2-year OS rates of TTI1 low group] 88.1% vs. [2-year OS rates of TTI1 high group] 82.3%, [5-year OS rates of TTI1 low group] 55.5% vs. [5-year OS rates of TTI1 high group] 40.7%, [2-year DFS rates of TTI1 low group] 85.5% vs. [2-year DFS rates of TTI1 high group] 63.5%, [5-year DFS rates of TTI1 low group] 49.3% vs. [5-year DFS rates of TTI1 high group] 23.3%, respectively; Figure 6A). The OS of the NSCLC Ki67 low group was higher than that of the Ki67 high group ($P = 0.0003$) in the 2-year and 5-year postoperative periods, and the Ki67 low group of NSCLC patients with DFS was significantly higher than that of the Ki67 high group ($P < 0.0001$) (Figure 6B). Subsequently, we analyzed the combined role of TTI1 and Ki67 in

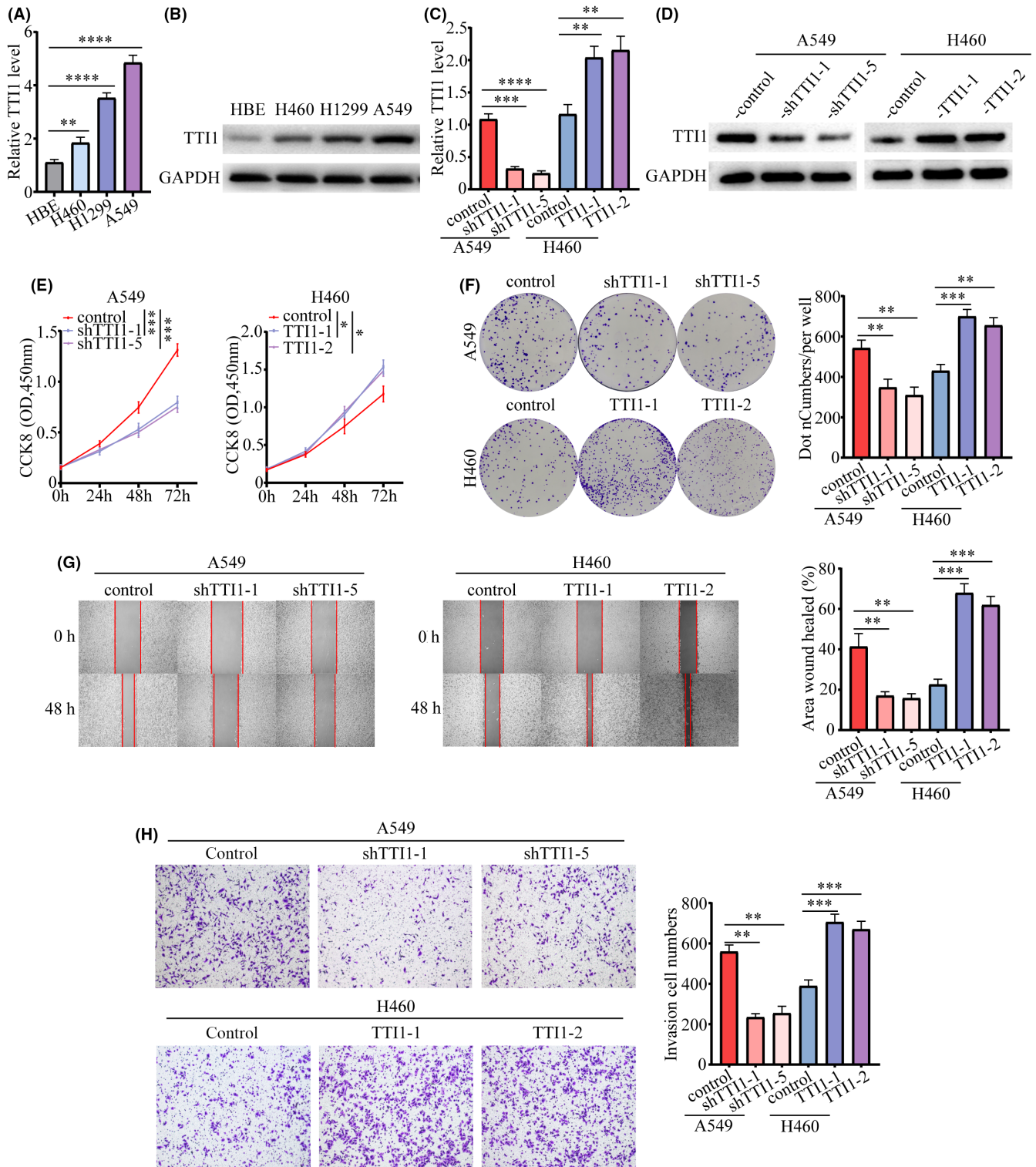


FIGURE 3 TELO2-interacting protein 1 (TTI1) knockdown or overexpression could alter the invasion, metastasis, and proliferation of non-small-cell lung cancer (NSCLC) cells in vitro. (A, B) The mRNA and protein expression levels of TTI1 in human bronchial epithelioid (HBE) cells and three NSCLC cell lines (H460, A549, and H1299) were detected respectively by qRT-PCR and western blot. (C, D) The transfection efficiency of four stable cell lines, H460-TTI1-1, H460-TTI1-2, and A549-shTTI1-1, A549-TTI1-5, was validated by quantitative real-time polymerase chain reaction and western blot. (E) The proliferation ability of H460-TTI1-1, H460-TTI1-2, and A549-shTTI1-1, A549-TTI1-5 cells was measured by CCK-8 assays. (F) The viability of H460-TTI1-1, H460-TTI1-2, and A549-shTTI1-1, A549-TTI1-5 cells was detected by colony formation assays. (G) The migration of H460-TTI1-1, H460-TTI1-2, and A549-shTTI1-1, A549-TTI1-5 cells was detected by wound healing assay. (H) The invasion ability of H460-TTI1-1, H460-TTI1-2, and A549-shTTI1-1, A549-TTI1-5 cells was detected by the Matrigel transwell assay. The data are presented as mean \pm SD, $n = 3$; ** $P < 0.01$, *** $P < 0.001$, **** $P < 0.0001$

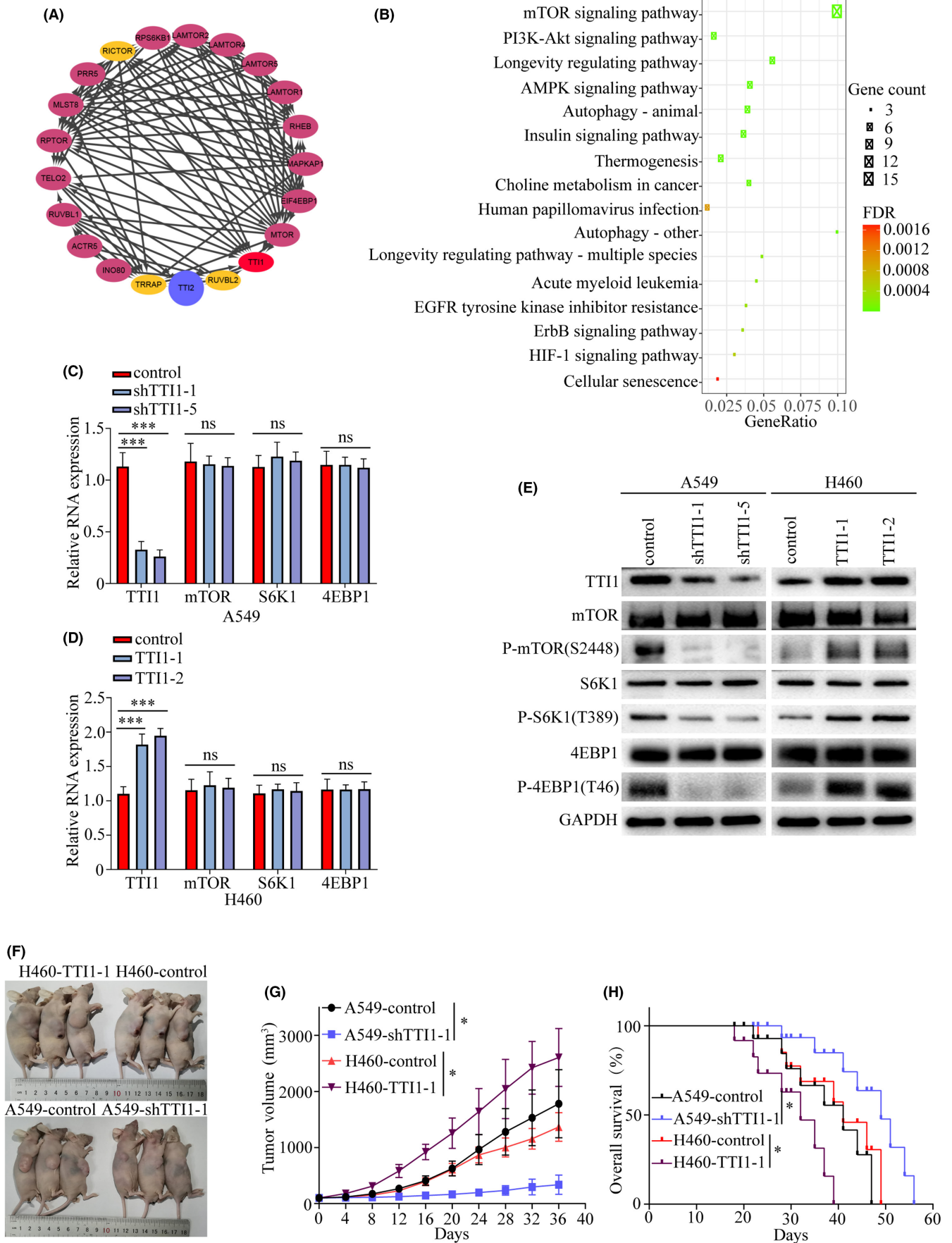


FIGURE 4 Legend on next page

FIGURE 4 TTI1 regulates the mTOR signaling pathway and promotes non-small-cell lung cancer (NSCLC) progression in vivo. (A) Protein-protein interaction networks about TTI1 from the STRING database. (B) The Kyoto Encyclopedia of Genes and Genomes analysis explores TTI1-related downstream pathways from the STRING database. (C, D) Quantitative real-time polymerase chain reaction detects TTI1, mTOR, and downstream signaling genes' mRNA levels, including S6K1 and 4EBP1. (E) Western blot analysis of TTI1, mTOR, p-mTOR, S6K1, p-S6K1, 4EBP1, and p-4EBP1 protein levels. (F) Image of harvested subcutaneous tumors that A549-shTTI1-1, H460-TTI1-1, and control cells were implanted into the nude mice. (G) The tumor volume was calculated every 4 days after it reached 100 mm³. (H) The prognosis of those nude mice subcutaneously implanted with A549-shTTI1, H460-TTI1, and negative control cells. The data are presented as mean \pm SD, $n = 3$; * $P < 0.05$, ** $P < 0.01$, *** $P < 0.01$; ns, not significant

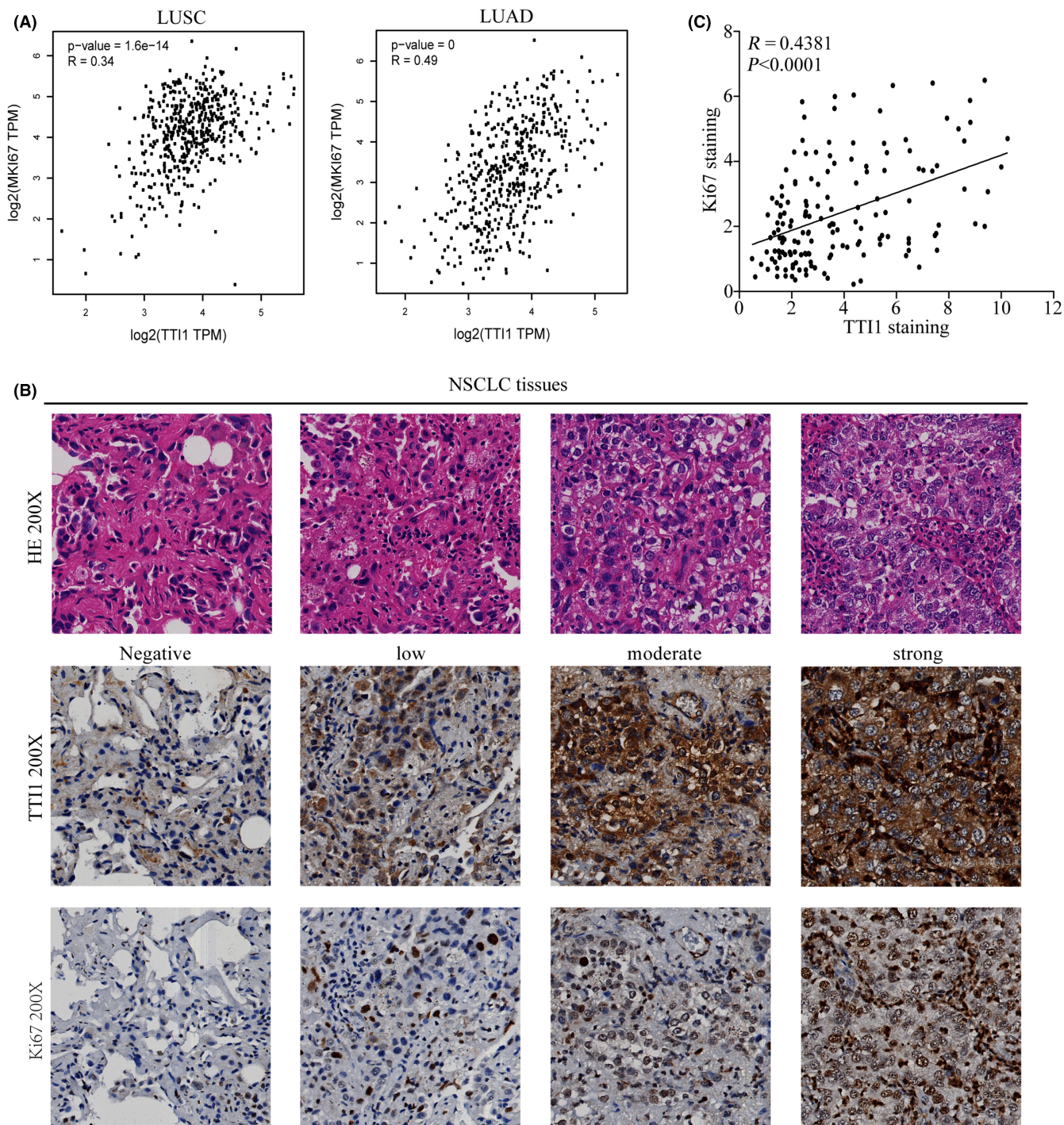
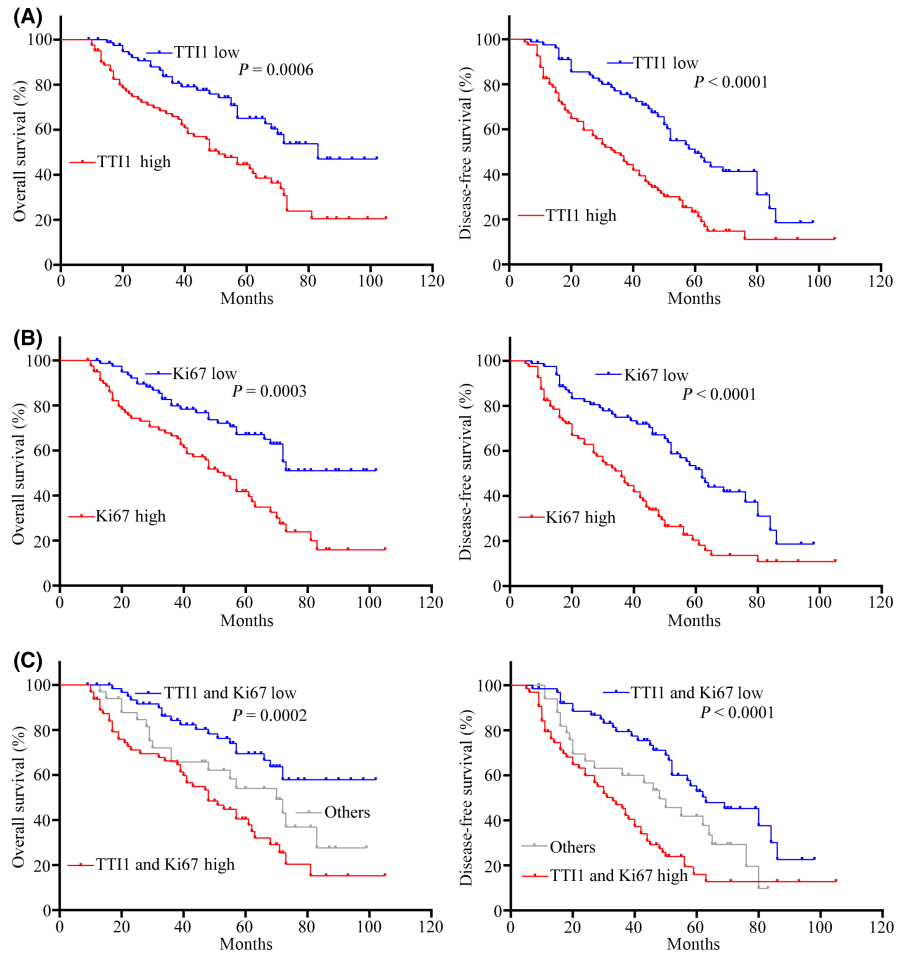


FIGURE 5 The expression of TTI1 and Ki67 in non-small-cell lung cancer (NSCLC) patients. (A) Pearson analysis of the correlation between TTI1 and Ki67 was conducted on GEPIA, with all data based on The Cancer Genome Atlas. (B) Representative images of TTI1 and Ki67 expression in NSCLC tissues of serial sections stained with H&E and immunohistochemistry. (C) Pearson analysis of the correlation between TTI1 and Ki67 expression in 160 paired NSCLC specimens. LUAD, lung adenocarcinomas; LUSC, lung squamous cell carcinomas

FIGURE 6 Prognostic significance of TELO2-interacting protein 1 (TTI1) and Ki67 in non-small-cell lung cancer (NSCLC) patients. Survival analysis of overall survival (OS) and disease-free survival (DFS) of 160 NSCLC patient groups according to the expression of TTI1 (TTI1^{high} vs. TTI1^{low}) was performed using Kaplan–Meier and log rank analysis. Survival analysis of OS and DFS of 160 NSCLC patient groups based on Ki67 expression (Ki67^{high} vs. Ki67^{low}). Survival analysis of OS and DFS of 160 NSCLC patient groups according to the expression of TTI1 and Ki67 (TTI1 and Ki67 high vs. TTI1 and Ki67 low vs. others).



OS and DFS. One hundred and sixty NSCLC patients were divided into three subgroups according to TTI1 and Ki67 expression levels: TTI1 high and Ki67 high, TTI1 low and Ki67 low, and others. The 2-year and 5-year OS and DFS rates in the TTI1 high and Ki67 high groups were significantly lower than those in the TTI1 low and Ki67 low groups and the others group (Figure 6C). These findings reveal that TTI1 or Ki67 could be a tumor biomarker for NSCLC, but TTI1 combined with Ki67 could be a better tumor biomarker for NSCLC.

4 | DISCUSSION

NSCLC is a devastating disease. Although the continuous improvement of treatment methods has reduced the death rate of NSCLC year by year,¹⁶ the overall cure and survival rates of patients with NSCLC are still very low,¹⁷ therefore further exploration of the mechanism of NSCLC oncogenesis, progression, and recurrence is necessary and exigent. Our study showed that TTI1 had significantly high expression in NSCLC specimens compared with noncancerous tissues, and high TTI1 expression was positively associated with large tumor size, advanced TNM stage, and lymph node metastasis. Furthermore, patients with high expression of TTI1 and Ki67 had poorer prognosis and higher recurrence than those with low levels

of TTI1 and Ki67. Importantly, we found that the combination of TTI1 and Ki67 was an independent parameter for predicting prognosis and recurrence in NSCLC patients. On this basis, we conclude that TTI1 serves as the facilitator of NSCLC progression, and TTI1 or TTI1 combined with Ki67 can be used to predict prognosis and recurrence in patients with NSCLC.

The TELO2-TTI1-TTI2 (TTT) complex can recognize newly synthesized PIKKs and transfer them to the R2TP complex (RUVBL1-RUVBL2-RPAP3-PIH1D1) and HSP-90 chaperone to support their folding and assembly.^{4,5} As members of the Ser/Thr kinase family, PIKKs play pivotal roles in various pathways related to cell metabolism, proliferation, and differentiation. All three proteins of the TTT complex form elongated helical repeat structures. TTI1 provides a platform on which TELO2 and TTI2 bind to its central region and C-terminal end, respectively,¹⁸ therefore TTI1 is a critical element for maintaining the stability and function of the TTT complex. TTI1 and TTI2 are also required for maintaining the protein levels of TEL2, and the triple T complex is required for DNA damage response signaling through control of the protein levels of ataxia telangiectasia mutated (ATM), ataxia-telangiectasia and Rad3-related (ATR), and a group of related PIKKs. TTI1 plays a pivotal role in DNA damage resistance, and studies prove that TTI1 depletion leads to significant DNA damage sensitivity.¹⁹

The activated mTOR signaling pathway is the key to promoting cell growth and plays a variety of roles in human cancer, including

cell survival, cytoskeleton rearrangement, invasion, metastasis, anti-apoptosis, and inhibition of autophagy.^{6,20-22} Recent studies have indicated that activated mTOR signaling could promote cancer cell proliferation, invasion, and metastasis.²³⁻²⁵ Kim et al. found that augmented mTORC1 signaling determines metastatic potential in renal cell carcinoma.²⁵ TTI1 and TTI2 are important for mTOR stability and activity.

Our study validated that overexpression of TTI1 could promote NSCLC cell proliferation, invasion, and metastasis in vitro and boosted NSCLC cell progression in vivo. However, the opposite result was obtained in NSCLC cells after TTI1 knockdown. Mechanistically, overexpression of TTI1 promotes phosphorylation of mTOR, S6K1, and 4EBP1. However, after TTI1 was knocked down, the levels of p-mTOR, p-S6K1, and p-4EBP1 decreased in NSCLC cells.

After the addition of mTOR kinase inhibitor AZD5088, the protein levels of p-mTOR, p-S6K1, and p-4EBP1 A549, A549-shTTI1-5, H460, and H460-TTI1-2 were all reduced compared with the DMSO treatment group. The viability and the proliferation, invasion, and migration capacity of those cells were all attenuated. Thus, our data revealed that TTI1 could regulate mTOR signaling activities. This explains why TTI1 can promote NSCLC proliferation, invasion, and metastasis. Moreover, TTI1 is positively associated with the expression of Ki67 in NSCLC tissues, and it was proved that TTI1 promotes NSCLC development via facilitating cell proliferation from another aspect.

The findings of our study suggest a pivotal oncogenic role of TTI1 in the progression of NSCLC and demonstrate an independent prognostic role of TTI1 in NSCLC. In terms of mechanism, TTI1 could regulate the mTOR signaling pathway. The expression of TTI1 and Ki67 had a good correlation in NSCLC, and the combination of TTI1 and Ki67 is a valuable biomarker for predicting the survival and recurrence of patients with NSCLC.

AUTHOR CONTRIBUTIONS

S.-Q.Z., L.-X.Z., and X.Y. conceived and designed the experiments. L.-X.Z., X.Y., and Z.-B.W. performed the experiments. Z.-M.L., D.-G.W., S.-W.C., F.L., and Y.-B.W. analyzed the data. L.-X.Z. and X.Y. wrote the paper. All authors read and approved the final manuscript.

ACKNOWLEDGMENTS

None.

FUNDING INFORMATION

This work was supported by the following grants: National Natural Science Foundation of China (81860520) and Department of Science and Technology of Jiangxi Province (20213BCJL22048).

CONFLICT OF INTEREST

The authors declare no conflict of interest.

DATA AVAILABILITY STATEMENT

All data in our study are available upon request.

ETHICS STATEMENTS

The ethical approval was provided by the Ethics Committee of The Second Affiliated Hospital of Nanchang University (NO. SYXK2015-0001), and written informed consent was obtained from each patient. Permit for animal studies: SYXX 2021-0004.

CONSENT FOR PUBLICATION

All authors gave their consent for publication.

ORCID

Yong-Bing Wu  <https://orcid.org/0000-0002-6703-9087>

Shu-Qiang Zhu  <https://orcid.org/0000-0002-4601-7399>

REFERENCES

- Sung H, Ferlay J, Siegel RL, et al. Global cancer statistics 2020: GLOBOCAN estimates of incidence and mortality worldwide for 36 cancers in 185 countries. *CA Cancer J Clin*. 2021;71(3):209-249.
- Ettinger DS, Wood DE, Aisner DL, et al. Non-small cell lung cancer, version 5.2017, NCCN clinical practice guidelines in oncology. *J Natl Compr Canc Netw*. 2017;15(4):504-535.
- Molina JR, Yang P, Cassivi SD, Schild SE, Adjei AA. Non-small cell lung cancer: epidemiology, risk factors, treatment, and survivorship. *Mayo Clin Proc*. 2008;83(5):584-594.
- Pal M, Muñoz-Hernandez H, Bjorklund D, et al. Structure of the TELO2-TTI1-TTI2 complex and its function in TOR recruitment to the R2TP chaperone. *Cell Rep*. 2021;36(1):109317.
- Takai H, Xie Y, de Lange T, Pavletich NP. Tel2 structure and function in the Hsp90-dependent maturation of mTOR and ATR complexes. *Genes Dev*. 2010;24(18):2019-2030.
- Murugan AK. mTOR: role in cancer, metastasis and drug resistance. *Semin Cancer Biol*. 2019;59:92-111.
- Kaizuka T, Hara T, Oshiro N, et al. Tti1 and Tel2 are critical factors in mammalian target of rapamycin complex assembly. *J Biol Chem*. 2010;285(26):20109-20116.
- Rao F, Cha J, Xu J, et al. Inositol pyrophosphates mediate the DNA-PK/ATM-p53 cell death pathway by regulating CK2 phosphorylation of Tti1/Tel2. *Mol Cell*. 2014;54(1):119-132.
- Fernández-Sáiz V, Targosz BS, Lemeer S, et al. SCFFbxo9 and CK2 direct the cellular response to growth factor withdrawal via Tel2/Tti1 degradation and promote survival in multiple myeloma. *Nat Cell Biol*. 2013;15(1):72-81.
- Pei X, Chen SW, Long X, et al. circMET promotes NSCLC cell proliferation, metastasis, and immune evasion by regulating the miR-145-5p/CXCL3 axis. *Aging (Albany NY)*. 2020;12(13):13038-13058.
- Qiu BQ, Zhang PF, Xiong D, et al. CircRNA fibroblast growth factor receptor 3 promotes tumor progression in non-small cell lung cancer by regulating Galectin-1-AKT/ERK1/2 signaling. *J Cell Physiol*. 2019;234(7):11256-11264.
- Camp RL, Dolled-Filhart M, Rimm DL. X-tile: a new bio-informatics tool for biomarker assessment and outcome-based cut-point optimization. *Clin Cancer Res*. 2004;10(21):7252-7259.
- Chresta CM, Davies BR, Hickson I, et al. AZD8055 is a potent, selective, and orally bioavailable ATP-competitive mammalian target of rapamycin kinase inhibitor with in vitro and in vivo antitumor activity. *Cancer Res*. 2010;70(1):288-298.
- Molina-Arcas M, Moore C, Rana S, et al. Development of combination therapies to maximize the impact of KRAS-G12C inhibitors in lung cancer. *Sci Transl Med*. 2019;11(510):eaaw7999.
- Holt SV, Logie A, Davies BR, et al. Enhanced apoptosis and tumor growth suppression elicited by combination of MEK (selumetinib) and mTOR kinase inhibitors (AZD8055). *Cancer Res*. 2012;72(7):1804-1813.

16. Siegel RL, Miller KD, Fuchs HE, Jemal A. Cancer statistics, 2021. *CA Cancer J Clin.* 2021;71(1):7-33.
17. Hirsch FR, Scagliotti GV, Mulshine JL, et al. Lung cancer: current therapies and new targeted treatments. *Lancet.* 2017;389(10066):299-311.
18. Kim Y, Park J, Joo SY, et al. Structure of the human Telo2-TTI1-TTI2 complex. *J Mol Biol.* 2021;434(2):167370.
19. Hurov KE, Cotta-Ramusino C, Elledge SJ. A genetic screen identifies the triple T complex required for DNA damage signaling and ATM and ATR stability. *Genes Dev.* 2010;24(17):1939-1950.
20. Wullschleger S, Loewith R, Hall MN. TOR signaling in growth and metabolism. *Cell.* 2006;124(3):471-484.
21. Mossmann D, Park S, Hall MN. mTOR signalling and cellular metabolism are mutual determinants in cancer. *Nat Rev Cancer.* 2018;18(12):744-757.
22. Zhou H, Huang S. Role of mTOR signaling in tumor cell motility, invasion and metastasis. *Curr Protein Pept Sci.* 2011;12(1):30-42.
23. Zhang X, Wang S, Wang H, et al. Circular RNA circNRIP1 acts as a microRNA-149-5p sponge to promote gastric cancer progression via the AKT1/mTOR pathway. *Mol Cancer.* 2019;18(1):20.
24. Yang C, Dou R, Wei C, et al. Tumor-derived exosomal microRNA-106b-5p activates EMT-cancer cell and M2-subtype TAM interaction to facilitate CRC metastasis. *Mol Ther.* 2021;29(6):2088-2107.
25. Kim K, Zhou Q, Christie A, et al. Determinants of renal cell carcinoma invasion and metastatic competence. *Nat Commun.* 2021;12(1):5760.

SUPPORTING INFORMATION

Additional supporting information can be found online in the Supporting Information section at the end of this article.

How to cite this article: Zhang L-X, Yang X, Wu Z-B, et al. TTI1 promotes non-small-cell lung cancer progression by regulating the mTOR signaling pathway. *Cancer Sci.* 2023;114:855-869. doi:[10.1111/cas.15668](https://doi.org/10.1111/cas.15668)